DEUTSCHES ELEKTRONEN-SYNCHROTRON DESY

DESY SR-78/10
July 1978

High Accuracy Bond Lengths from EXAFS of solid $KMnO_4$ and MnO_4^- in aqueous Solution

by

P. Rabe, G. Tolkiehn, A. Werner,
Institut für Experimentalphysik, Universität Kiel, Germany

NOTKESTRASSE 85 · 2 HAMBURG 52

To be sure that your preprints are promptly included in the
HIGH ENERGY PHYSICS INDEX ,
send them to the following address (if possible by air mail) :

DESY
Bibliothek
Notkestrasse 85
2 Hamburg 52
Germany

High accuracy bond lengths from EXAFS of solid $KMnO_4$ and MnO_4^- in aqueous solution

P Rabe, G Tolkiehn, and A Werner, Institut für Experimentalphysik, Universität Kiel, Germany

classification numbers: 61.10, 78.70 D

Abstract

Bond lengths and coordination numbers of the nearest neighbours of the central Mn atom in solid $KMnO_4$ and MnO_4^- in a 0.4 molar aqueous solution have been determined from the extended x-ray absorption finestructure (EXAFS) above the Mn K-edge. In the solution we find one shell of 4 oxygen atoms with a distance of 0.1649± 0.0005 nm from the central Mn atom.

In crystalline $KMnO_4$ we observe a beating in EXAFS due to the superposition of contributions from two close lying shells. A comparison of the phases and envelope functions of EXAFS of $KMnO_4$ and MnO_4^- yields a separation of 0.0125± 0.0003 nm for these shells. With the bond length in the solution we find three closer oxygen atoms at a distance of 0.1634± 0.0008 nm and one more distant atom at 0.1759± 0.0008 nm.

1. Introduction

In x-ray absorption spectra of polyatomic systems a finestructure is observed which extends to several hundred electronvolts above the absorption edges. This extended x-ray absorption finestructure (EXAFS) is due to a superposition of an outgoing photoelectron wave with an electron wave backscattered from the neighbouring atoms at the site of the absorbing atom. The periodicity and the amplitude of this finestructure reflect the parameters of the local ordering around the central atom, i.e. bond lengths and coordination numbers (Stern 1974, Lytle et al 1975, Stern et al 1975). From experimental EXAFS spectra bond lengths have been determined with accuracies up to 0.001 nm (Martens et al 1978).

After proposing the investigation of EXAFS as a tool for structural analysis the method has profitted from several recent instrumental and theoretical developments:

1.) Limitations of this method due to low intensities of the bremsstrahlung and the appearance of characteristic lines in the spectra of conventional x-ray sources have been overcome since synchrotron radiation became available for spectroscopic uses. At sufficient high electron energies the brightness of synchrotron radiation surmounts that of the continuous radiation of even the most powerful x-ray tubes by several orders of magnitude. Therefore high quality data can be obtained in short times (Eisenberger et al 1975).

2.) The accuracies for the determination of bond lenghts are dircetly connected with the precision of the scattering phases of the electron waves. These phases consider the influence of the absorbing and scattering atomic potentials on the electron wave (Stern 1974, Lee and Beni 1977). The dependence of the phases on the electron energy is characteristic for the absorbing and scattering atom pair. The chemical state of these atoms only plays a role in the range of low kinetic energies of the electrons. It has been shown that the phases can be extracted from experimental spectra of compounds with known geometrical structure and that these can be transferred to the same kind of atom pairs in systems of unknown geometry (Citrin et al 1976, Martens et al 1978).

In this paper we make use of this transferability of scattering phases. We shall show that bond lengths can be determined with high precision even when the scattering phases are extracted from and applied to atom pairs in different chemical environment. Further the precision can be increased if the chemical state of the atom pairs are identical.

2. Experiment

The spectra presented in this paper have been measured with the experimental setup shown in Fig. 1. The synchrotron-radiation of the Deutsches Elektronen-Synchrotron is monochromatized by a channelcut Ge-crystal. The surfaces of the crystal are cut parallel to the atomic planes {111} for which the even order reflections are suppressed according to a vanishing structure factor. In the energy range under consideration (6500 eV to 7500 eV) the spectral resolution amounts to 1 eV. The intensities of the monochromatic radiation are monitored by two air-filled ionization chambers. The signals are digitized and stored in a computer.

With this arrangement we obtain an effective reduction of the influence of intensity fluctuations on the absorption coefficient. The computer controls the position of the goniometer and of sample and detectors which are mounted on a lifting table. The solid samples are prepared from fine grain polycrystalline powder on adhesive tape. Special care was taken to produce homogeneous films to avoid distortion in the spectra. The 0.4 molar aqueous solution was kept between Mylar foils. The thickness of the samples has been chosen to give good contrast in the spectra but has not been determined explicitly. All spectra have been taken at room temperature.

3. Results and discussion

The contributions to the total absorption coefficient of $KMnO_4$ and MnO_4^- in solution due to excitations of Mn K-electrons are shown in Fig. 2. The monotonous background caused by excitations of weaker bound electrons has been removed by extrapolating the absorption coefficient in front of the K-edge to energies beyond the edge. The onset of the K-shell excitations is dominated by a sharp absorption line which appears in both cases at the same energy within the experimental error of 0.2 eV. This structure which is produced by transitions to a localized molecular orbital in the MnO_4^- ion (Rabe et al 1978) has been used to calibrate the energy scale relative to some characteristic lines of a conventional x-ray tube. Just above the edge up to $h\nu$ = 6600 eV the finestructures of the spectra differ significantly. In this region many-body interactions and density of states effects influence the transition probabilities (Stern 1974). These near edge structures are generally omitted when geo-

metrical structure informations are extracted from absorption spectra.

Beyond $h\nu$ = 6600 eV EXAFS shows up in the spectra which can be described by

$$(1) \qquad \chi(k) = -\frac{1}{k} \sum_i A_i(k) \sin(\varphi_i(R_i,k))$$

with

$$(2) \qquad A_i(k) = \frac{N_i}{R_i^2} \left| f_i(\pi,k) \right| e^{-2\sigma_i^2 k^2} e^{-2R_i/\lambda}$$

Here k denotes the wavenumber of the photoelectrons. The envelope function $A_i(k)$ of each shell, i.e. of the ensemble of N_i atoms at a distance R_i from the absorbing atom, is formed by the backscattering amplitude $|f(\pi, k)|$ the k-dependence of which is characteristic for the scattering atoms. σ_i^2 and λ consider the influence of thermal vibrations and scattering of electrons to incoherent states respectively. Bond lengths can be calculated from

$$(3) \qquad \varphi_i(R_i,k) = 2kR_i + \Phi_i(k)$$

where $\Phi_i(k)$ is the scattering phase of the photoelectron wave.

The finestructures $\chi(k)$ extracted from our experimental data by removing the monotonous background of K-shell absorption are shown in Fig. 3, curves a and b. In both cases the position of the sharp absorption line in front of the K-edge ($h\nu$ = 6541 eV) has been taken as zero for the conversion of the energy scale to the k-scale. Using a Gaussian window function

(Martens et al 1978) the range from $33nm^{-1}$ to $130nm^{-1}$ has been Fourier transformed to real space. The magnitude of the Fourier transforms $|F(r)|$ i.e. the radial structure functions are shown in Fig. 3 curves c and d. In both cases $|F(r)|$ is dominated by a peak at r = 0.13nm which is caused by the oxygen atoms surrounding the central Mn atom. Note that the amplitudes in $|F(r)|$ as well as in $\chi(k)$ are smaller in the case of $KMnO_4$ as compared to the solution. This points to differences in the geometrical structure, and will be discussed later.

Compared to the true distances the peaks in $|F(r)|$ are shifted by the k dependent parts of the scattering phases. To calculate bond lengths the phases $\Phi_i(k)$of the Mn-O atom pair has been extracted from an experimental Mn K-absorption spectrum of MnO_2 (Fig. 4a). From the oscillating part of the absorption coefficient (Fig. 4 b) the radial structure function $|F(r)|$ has been calculated (Fig. 4c). The first prominent peak at r = 1.5 Å is due to the first oxygen scattering shell. Due to our transformation window the informations about $\chi(k)$ of a single scattering shell are concentrated within a limited range in real space as indicated by bars in Fig. 3 curves c and d and Fig. 4 curve c. From the real and imaginary parts of a backtransform of these ranges we have calculated φ_{MnO_2} and $\varphi_{MnO_4^-}$. These functions have been used for calculation of the Mn-O distance in MnO_4^-. According to the transferability of phases Φ_{MnO_2} and $\Phi_{MnO_4^-}$ in equ.3 are assumed to be the same in both cases. Then the difference of the Mn-O bond lengths in MnO_2 and MnO_4^- can be calculated from

$$\Delta R(k) = (\varphi_{MnO_2} - \varphi_{MnO_4^-}) / (2k) \qquad (4)$$

This function should be a constant over the whole measured k-space. The most uncertain parameter for the calculation of ΔR is the zero of the kinetic energy E_o of the photoelectrons. Therefore E_o has to be varied in equ. 4 to obtain a constant ΔR over a large spectral range when experimental scattering phases are used (Martens et al 1978). This variation certainly compensates the greater part of changes of the scattering phases at low kinetic energies of the photoelectrons. With an energy shift of ΔE = -15 EV for MnO_2 relative to the absorption line in MnO_4^-, i.e. E_o = 6527 eV we obtain a k-dependence of ΔR as shown in Fig. 5. Around an average value of ΔR = 0.0231nm this function varies by less than $\pm 5 \cdot 10^{-4}$nm. Together with the Mn-O-distance of 0.188nm in MnO_2 (Wyckoff 1968) we obtain an absolute Mn-O bond length in MnO_4^- of 0.1649 ±0.0005nm.

The amplitude functions A(k) of the first scattering shell of MnO_2 and MnO_4^- calculated from the backtransform have been used to check the coordination numbers. The ratio $N_{MnO_4^-}/N_{MnO_2}$ can be calculated from

$$\ln(A_{MnO_4^-}/A_{MnO_2}) = 2\Delta\sigma^2 k^2 + 2\Delta R/\lambda + \ln\left[\frac{N_{MnO_4^-}}{N_{MnO_2}} \left(\frac{R_{MnO_2}}{R_{MnO_4^-}}\right)^2\right] \qquad (5)$$

with

$$\Delta\sigma^2 = \sigma^2_{MnO_2} - \sigma^2_{MnO_4^-} \qquad (6)$$

The result plotted vs k^2 is shown in Fig. 6. The deviations from a straight line at the boundaries of the shown k^2-region are caused by window effects in the Fourier transform. The intersection with the vertical axis obtained from an extrapolation

of the linear range determines the relative coordination numbers. Assuming 6 atoms in the first shell of MnO_2 (Wyckoff 1968) and a mean free path of the electrons of $\lambda = 0.6 \pm 0.2$nm (Stern et.al 1975) we obtain $N_{MnO_4^-} = 4.05 \pm 0.10$. From the slope of the straight line we calculate an increase of the mean square relative displacement of $\Delta\sigma^2 = 4 \times 10^{-5} nm^2$ in going from MnO_4^- to MnO_2.

The same procedure has been applied to determine bondlengths and coordination numbers in $KMnO_4$. In calculating $\Delta R(k)$ from equ.4 φ_{MnO_2} and $\varphi_{MnO_4^-}$ have been replaced by $\varphi_{MnO_4^-}$ and φ_{KMnO_4} respectively. In going from MnO_4^- to $KMnO_4$ the chemical environment of the Mn atoms is preserved so that there is no reason to vary E_o. In both cases E_o has been fixed at the absorption line in front of the edges. The result for $\Delta R(k)$ presented in Fig. 7 shows a significant k dependence which can be explained with a beating in EXAFS (Martens et al 1977): For two shells occupied with the same type of scattering atoms we can replace equ. 1 by

$$\chi(k) = \tilde{A}(k) \cdot \sin(2k\tilde{R} + \tilde{\Phi}(k)) \tag{7}$$

with

$$\tilde{A}(k) = A_1(k) \left(1 + c^2 + 2c \cos(2\Delta Rk)\right)^{1/2} \tag{8}$$

and

$$\tan\tilde{\Phi}(k) = \frac{\sin(\Phi - \Delta Rk) + c \sin(\Phi + \Delta Rk)}{\cos(\Phi - \Delta Rk) + c \cos(\Phi + \Delta Rk)} \tag{9}$$

Here $c = A_2 / A_1$ is the ratio of the envelope functions, $\tilde{R} = (R_1 + R_2)/2$ the average distance of the scattering atoms from the central atom and $\Delta R = R_2 - R_1$. Assuming two oxygen shells in $KMnO_4$ the equ. 4 can be replaced by

$$D(k) = \Delta\bar{R} - \frac{1}{2k}\tan^{-1}\left(\frac{c-1}{c+1}\tan(\Delta Rk)\right) \tag{1o}$$

where $\Delta\bar{R}$ is the difference between the Mn-O bond length in MnO_4^- and the average Mn-O bond length in $KMnO_4$. We have fitted our experimental data (Fig. 7) with equ. 1o. The parameter c is confined to three values due to the three possible relative occupation numbers. For fixed c the k dependent parts of D(k) are determined by the single parameter ΔR. The result of our fit is included in Fig. 7. With $\Delta\bar{R} = 0.0047$nm, $c = 0.28$ and $\Delta R = 0.0125$nm the calculated values follow the experimental curve within 10^{-4}nm. A variation of ΔR by 5×10^{-4}nm results in a significant deviation of the theoretical values from the experimental curve. We can restrict the uncertainty for $\Delta\bar{R}$ and ΔR to ± 0.0003nm. Together with the Mn-O bond length determined above we can calculate the absolute bond lengths in $KMnO_4$: Our investigation yields distances of (0.1634 ± 0.0008) nm for three oxygen atoms and (0.1759 ± 0.0008) nm for one oxygen atoms. This result is supported by the difference in the amplitudes of $\chi(k)$ and $|F(r)|$ for $KMnO_4$ and MnO_4^-. According to equ. 8 the amplitude of $\chi(k)$ is reduced when the splitting of a scattering shell into two close lying shells leads to a beating in EXAFS.

Bond lengths in $KMnO_4$ have been reported by Pallnik (1967). He finds an Mn-O distance of (0.1629 ± 0.0008) nm which is in excellent agreement with one of our values.

Our results show that bond lengths and coordination numbers in close lying shells can be determined with high precision by analysing the beating in EXAFS. This method

offers new possibilities for the analysis of geometrical structures in complex systems where small changes of bond lengths are expected.

This work was supported by the Bundesministerium für Forschung und Technologie (BMFT) and the Deutsches Elektronen-Synchrotron (DESY). The support of the experiment by Prof. R. Haensel is gratefully acknowledged.

References

Citrin P H , Eisenberger P and Kincaid B M 1976
Phys. Rev. Letters 36, 1346 - 1349

Eisenberger P and Kincaid B M 1975
Chem. Phys. Letters 36, 134 - 136

Lee P and Beni G 1977
Phys. Rev. B15, 2862 - 2883

Lytle F W , Sayers D E and Stern E A 1975
Phys. Rev. B11, 4825 - 2835

Martens G , Rabe P , Schwentner N and Werner A 1977
Phys. Rev. Letters 39, 1411 - 1414

Martens G , Rabe P ,Schwentner N and Werner A 1978
Phys. Rev. B17, 1481 - 1488

Pallnik G J 1967
Inorg. Chem. 6, 5o7 - 5o8

Rabe P , Tolkiehn G and Werner A 1978
to be published

Stern E A 1974
Phys. Rev. B1O, 3o27 - 3o37

Stern E A , Sayers D E and Lytle F W 1975
Phys. Rev. B11, 4836 - 3846

Wyckoff R W 1968 Crystal Structures
(New York: Interscience Publishers)

Figure Captions

Figure 1: Experimental setup
LS leadslit; CR crystal; IC ionization chamber;
S sample; GO goniometer; LT lifting table drive;
C current amplifier; VC voltage-to-frequency converter;
SC signal counter; RC reference counter

Figure 2: Absorption spectra of $KMnO_4$ and MnO_4^- in aqueous solution

Figure 3: EXAFS (a and b) and magnitude of the Fourier transform (c and d) of $KMnO_4$ and MnO_4^-

Figure 4: Absorption spectrum (a), EXAFS (b), and magnitude of the Fourier transform (c) of MnO_2

Figure 5: Difference in Mn-O bond lengths of MnO_2 and MnO_4^- determined from experimental data using equ. 4

Figure 6: Determination of relative coordination numbers and differences of mean square relative displacements in MnO_2 and MnO_4^- using equ. 5

Figure 7: D(k) for $KMnO_4$ and MnO_4^- (solid line: determined from experimental data with equ. 4; crosses: calculated from equ. 1o)

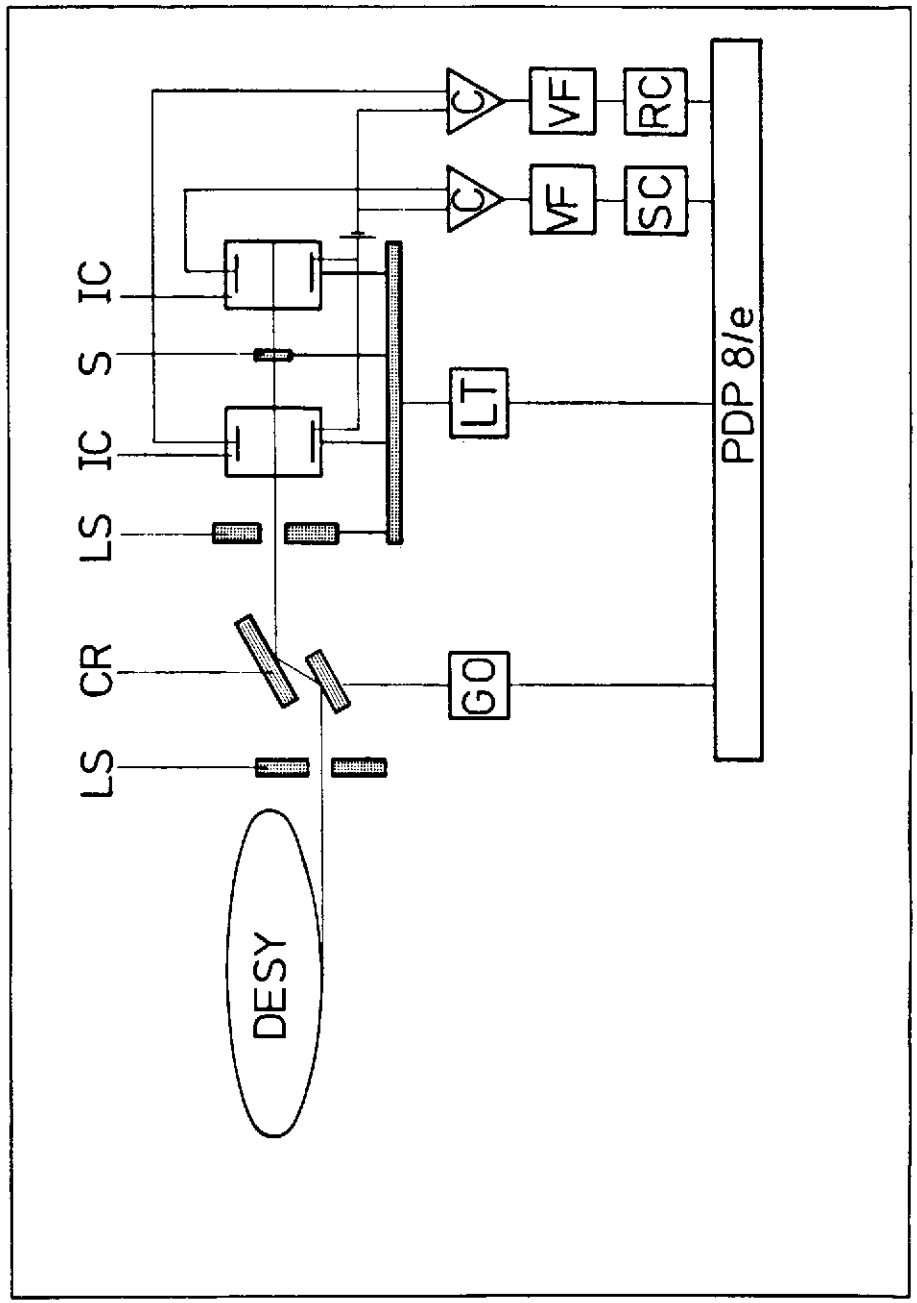

Fig. 1

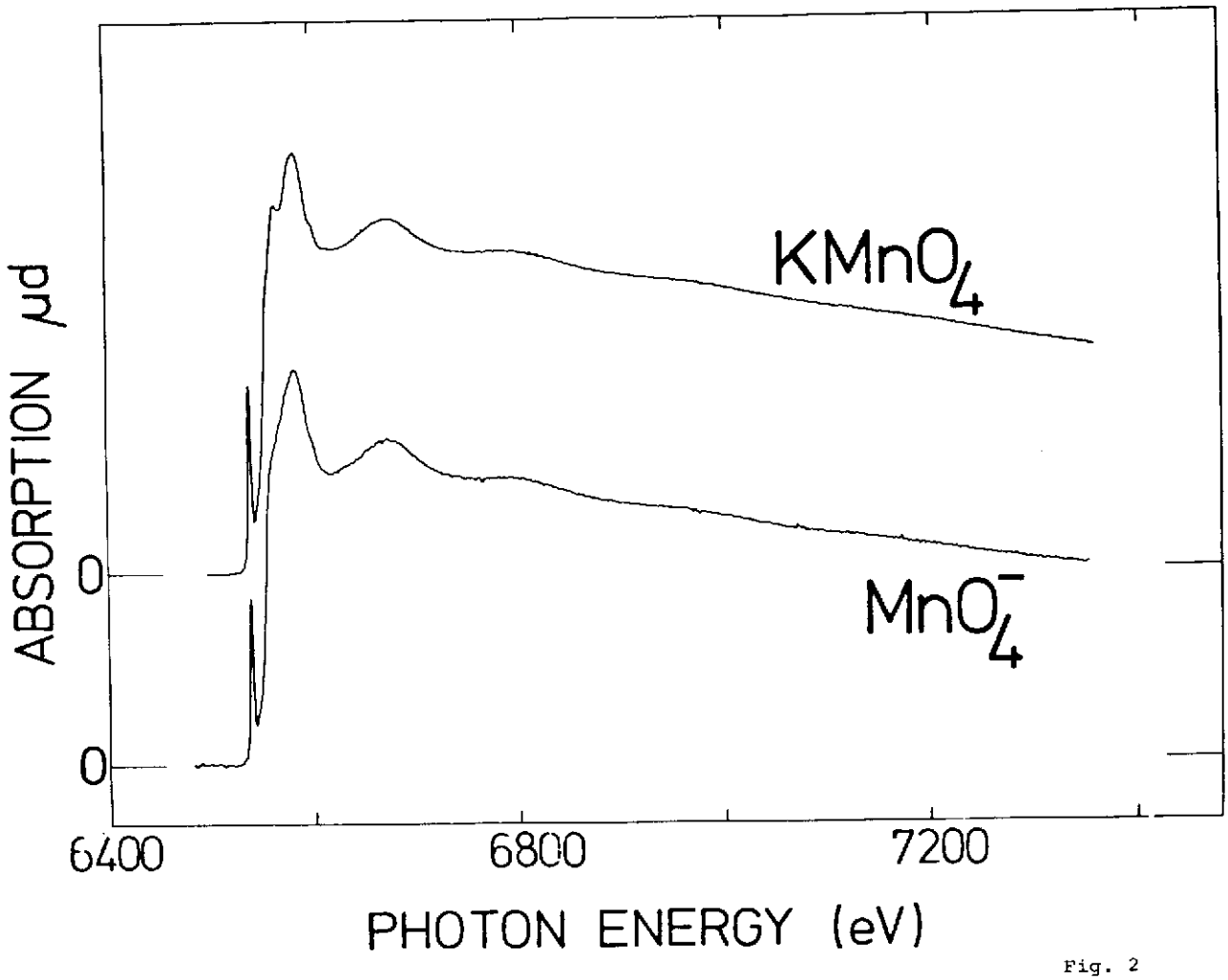
KMnO4
MnO4-
ABSORPTION μd
0
0
6400
6800
7200
PHOTON ENERGY (eV)

Fig. 2

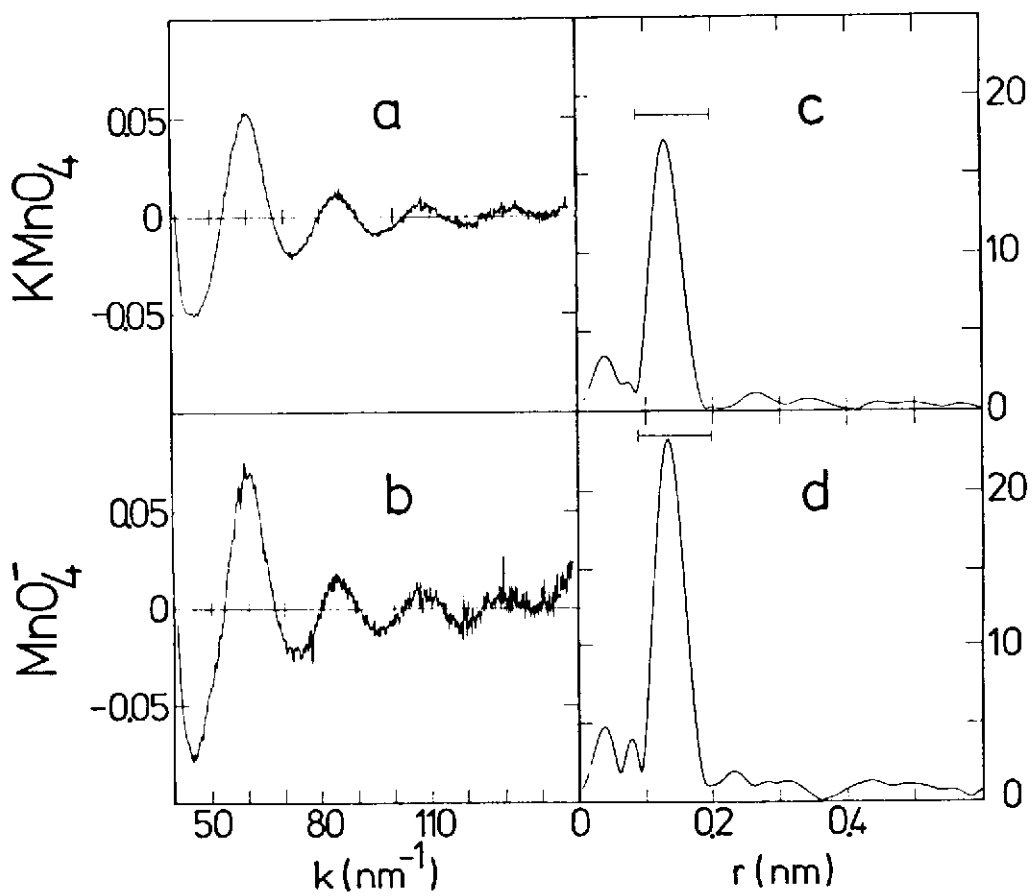
χ (k)
|F(r)|
KMnO4
MnO4-
a
b
c
d
0.05
0
-0.05
20
10
0
50
80
110
0
0.2
0.4
k (nm-1)
r (nm)

Fig. 3

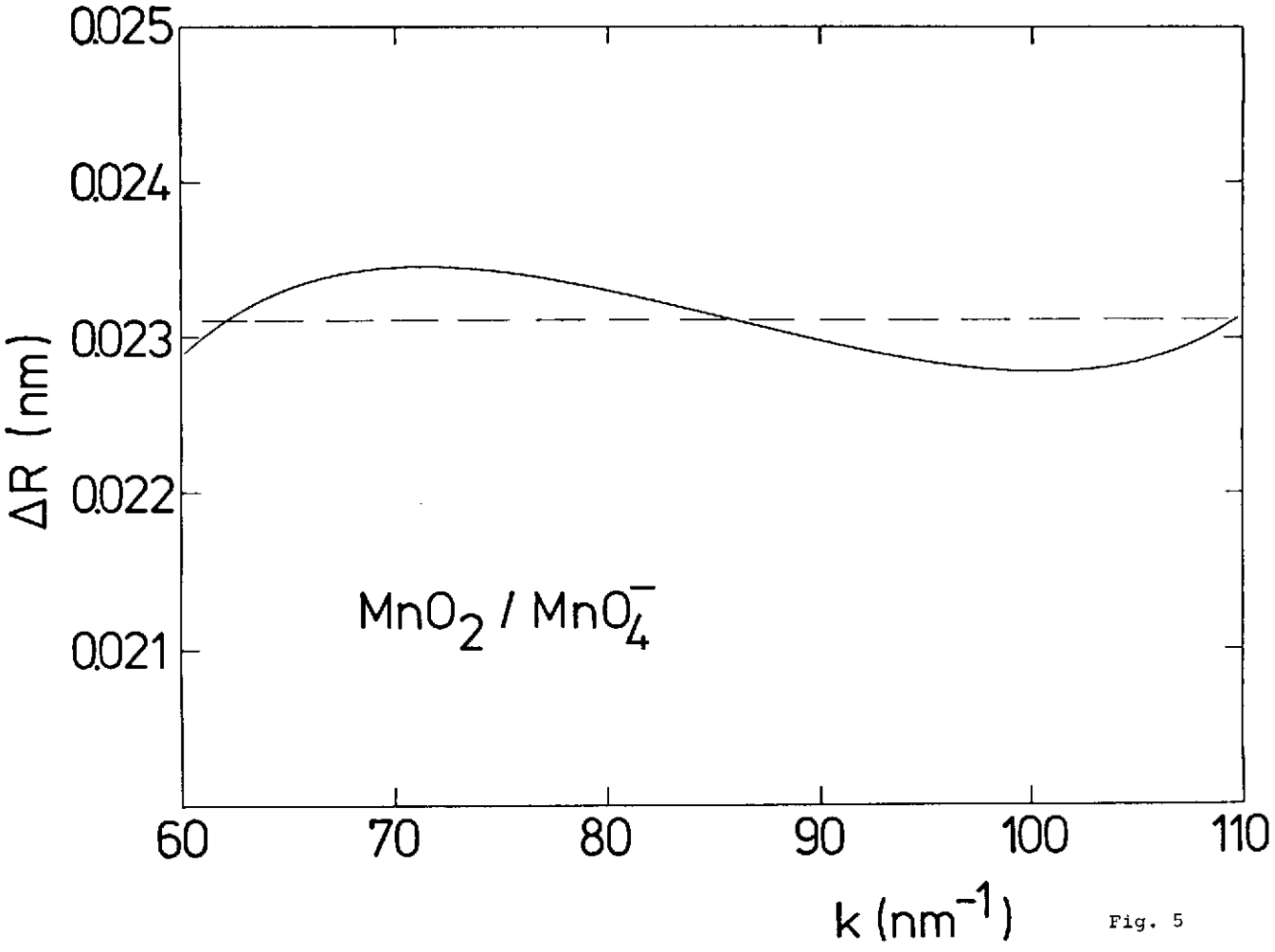
0.025
0.024
0.023
0.022
0.021
ΔR (nm)
MnO_2 / MnO_4^-
60
70
80
90
100
110
k (nm^{-1})

Fig. 5

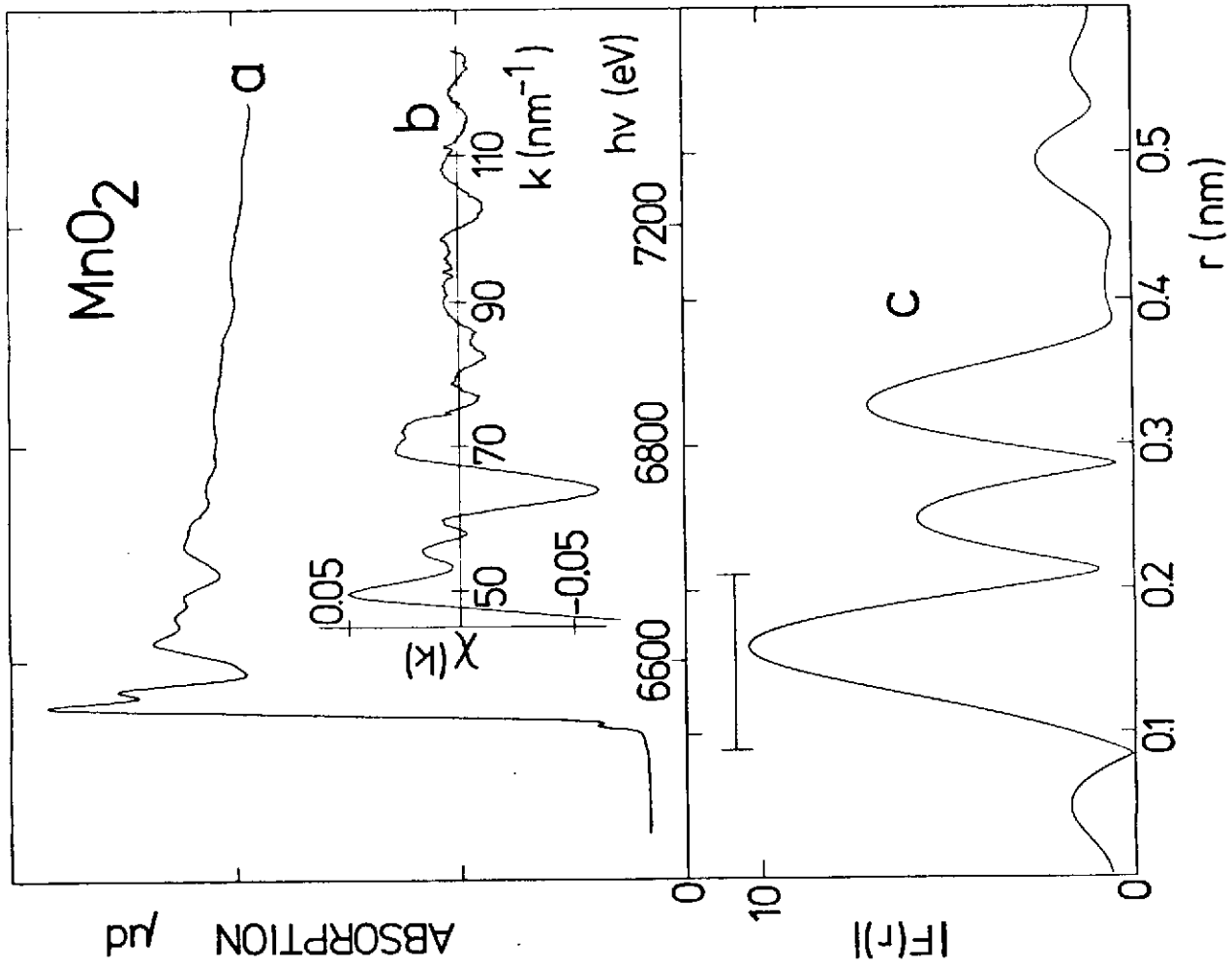
MnO_2
a
b
c
hν (eV)
6600
6800
7200
k (nm^{-1})
50
70
90
110
0.05
-0.05
χ(k)
ABSORPTION
μd
|F(r)|
r (nm)
0
0.1
0.2
0.3
0.4
0.5
10

Fig. 4

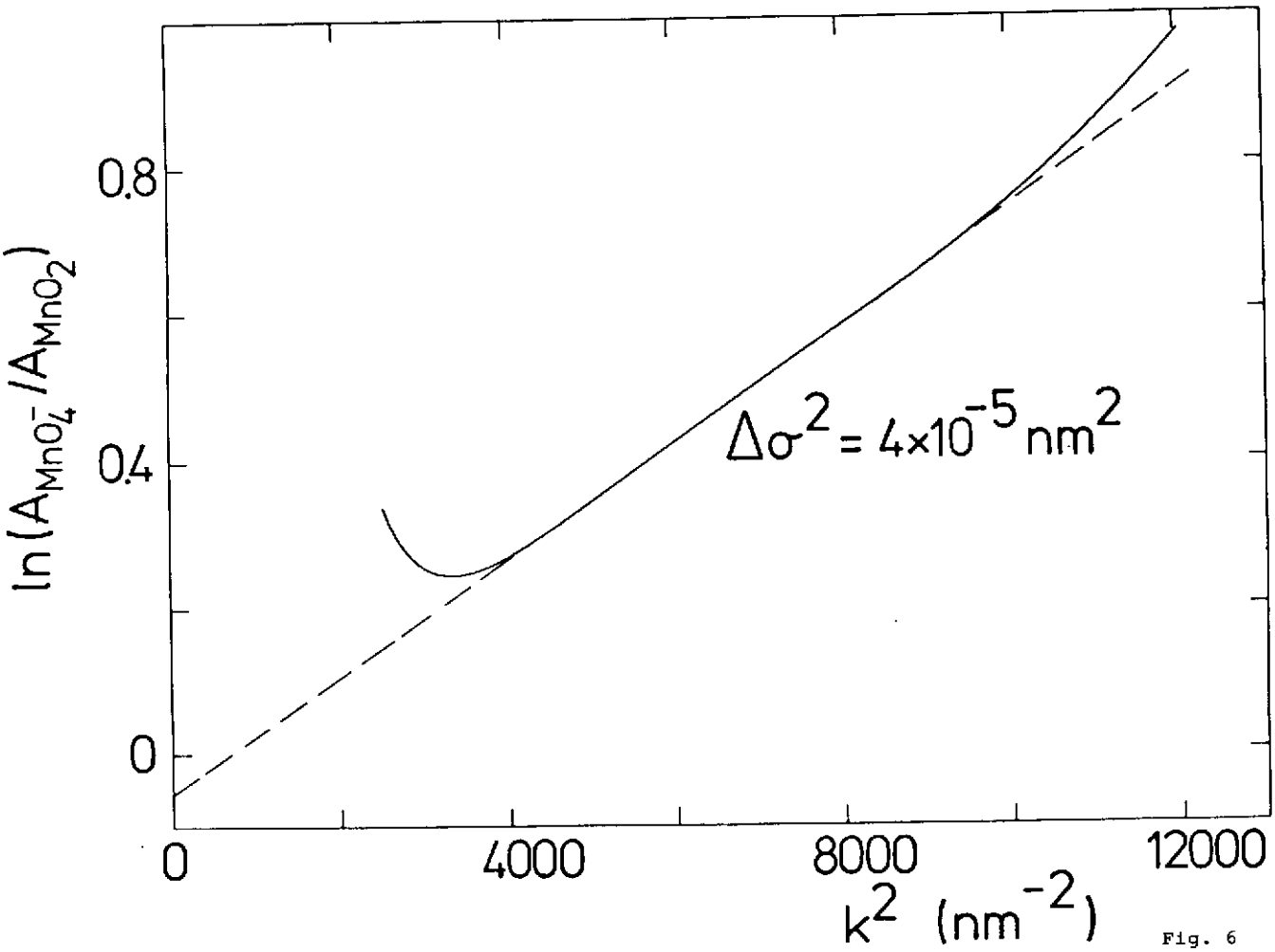
0.8
0.4
0
$\ln(A_{MnO_4^-}/A_{MnO_2})$
$\Delta\sigma^2 = 4\times10^{-5}\,nm^2$
0
4000
8000
12000
k^2 (nm^{-2})

Fig. 6

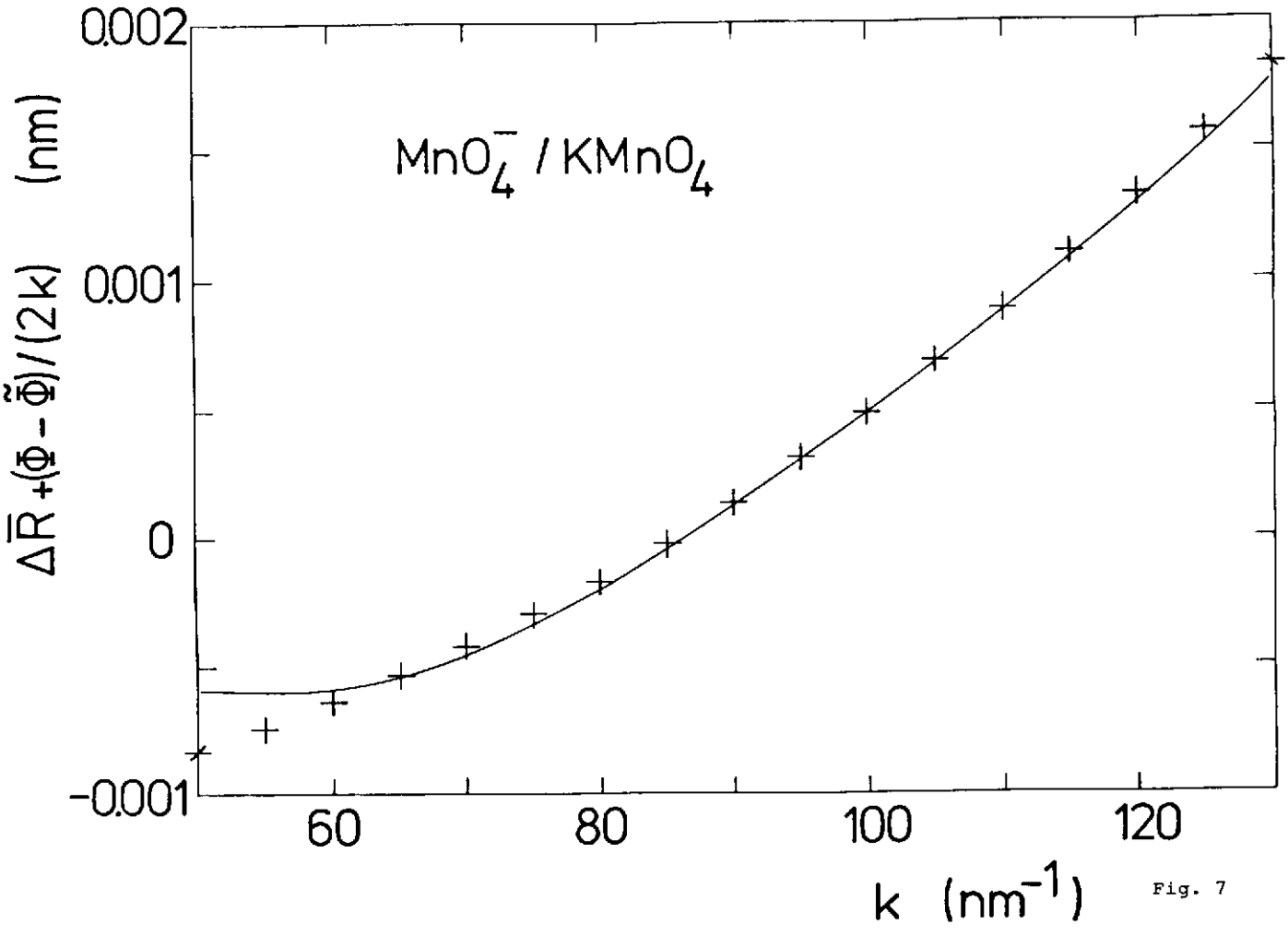
0.002
0.001
0
-0.001
$\Delta\bar{R} + (\Phi - \tilde{\Phi})/(2k)$ (nm)
MnO_4^- / $KMnO_4$
60
80
100
120
k (nm^{-1})

Fig. 7